Variations of North Atlantic inflow to the central Arctic Ocean over the last 14 million years inferred from hafnium and neodymium isotopes

Tian-Yu Chen [a,*], Martin Frank [a], Brian A. Haley [b], Marcus Gutjahr [c], Robert F. Spielhagen [a,d]

[a] Helmholtz Centre for Ocean Research Kiel (GEOMAR), Wischhofstrasse 1-3, 24148 Kiel, Germany
[b] CEOAS, Oregon State University, 104 CEOAS Admin. Bldg., Corvallis, OR, 97331-5503, USA
[c] Ocean and Earth Sciences, National Oceanography Centre, University of Southampton, Southampton, UK
[d] Academy of Sciences, Humanities and Literature, 55131 Mainz, Germany

ARTICLE INFO

ABSTRACT

The warm and saline North Atlantic inflow to the Arctic Ocean is a major component of high northern latitude circulation and the main mechanism of deep water renewal in the Arctic Ocean. Knowledge of its past variability is critical for understanding the high latitude feedback mechanisms of the climate system. Here we present the first combined seawater Hf and Nd isotope compositions of past Arctic Intermediate Water extracted from the authigenic Fe–Mn oxyhydroxide fraction of two sediment cores recovered near the North Pole, to reconstruct changes in contributions from glacial brines of the Eurasian shelf and past inflow of Atlantic waters. The Hf and Nd isotopic compositions obtained from leachates of the authigenic fraction show closely coupled and environmentally controlled variations over the past 14 million years. An observed offset of these data from seawater ε_{Hf} and ε_{Nd} compositions from other ocean basins (seawater array) is interpreted as the result of continuously prevailing glacial weathering conditions on the high latitude Eurasian continent. In the late Quaternary, large amplitude Hf and Nd isotopic variations of Arctic Intermediate Water (AIW) was characterized by more radiogenic isotope signatures generally prevailing under glacial conditions and less radiogenic values during interglacial periods. On the basis of the close coupling between Nd and Hf isotopes, we suggest that the evolution of Hf isotope compositions of central Arctic AIW has primarily been controlled by changes in ocean circulation and provenance of weathering inputs, rather than changes in weathering regime.

© 2012 Elsevier B.V. All rights reserved.

1. Introduction

Water mass exchange between the North Atlantic and the Arctic Ocean strongly affects heat and salinity distribution in the Arctic Ocean and thus the climate of the circum-Arctic continental regions (e.g., Aagaard et al., 1985; Rudels et al., 1994; Zhang et al., 1998). It has been demonstrated that modern heat transfer to the Arctic through Atlantic water inflow is significantly enhanced, which is most likely related to the Arctic amplification of global warming (Spielhagen et al., 2011). Therefore, knowledge of past variability of North Atlantic inflow to the Arctic is important for understanding the feedback mechanisms with the local and global climate system, as well as for predicting future changes. Until now, studies on the history of North Atlantic inflow are still rare and have focused on sediment records covering the last two glacial cycles at best (e.g., Spielhagen et al., 2004), whereas information on the evolution of the central Arctic basin and further back in time is still limited. Presently, inflowing North Atlantic water is transformed into Arctic intermediate waters, which remain largely decoupled from the atmosphere after entering the Arctic Ocean through Fram Strait and the Barents Sea (Fig. 1, Rudels et al., 1994; Karcher and Oberhuber, 2002). The central Arctic Intermediate Water (AIW) occupies water depths between 200 and 1,500 m and predominantly consists of these waters of North Atlantic origin. Major present-day modifications of AIW include interactions with brine water ejected by seasonal sea-ice production on the shallow Barents and Kara Sea shelves (e.g., Andersson et al., 2008). In the Eurasian Basin (Amundsen Basin and Nansen Basin), the topographically constrained cyclonic circulation brings the intermediate water back towards the Fram Strait along the Lomonosov Ridge (Fig. 1). A change of the inflow of Atlantic water will thus be directly reflected by corresponding changes of the chemical composition of AIW. In turn, the study of past compositions of AIW in the central Arctic basin will provide essential information about the temporal variability of the Atlantic inflow.

Combined radiogenic Hf–Nd isotope compositions of seawater were suggested as a proxy for changes in water mass provenance
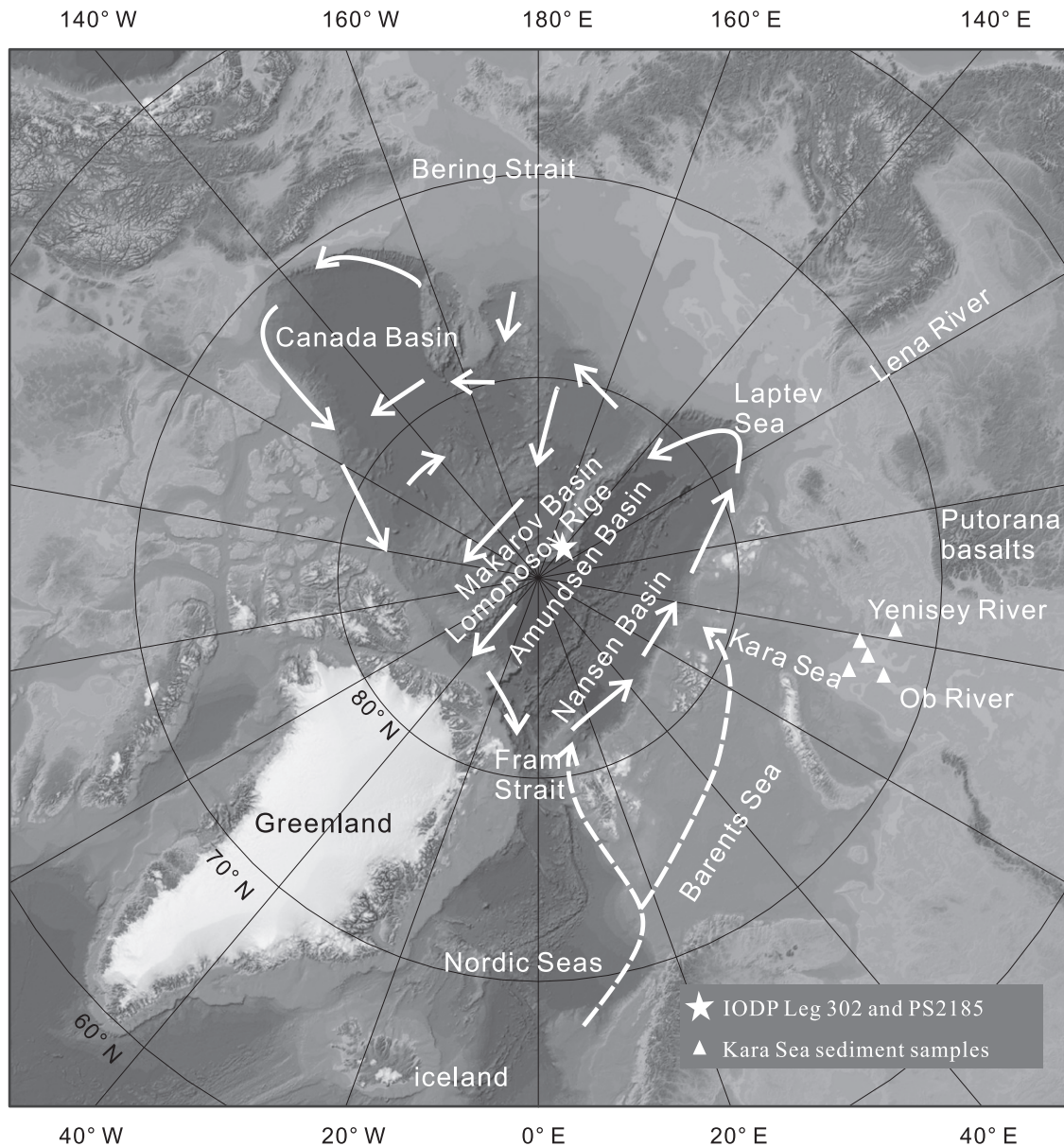
Fig. 1. Map of the high northern latitude seas and schematic modern ocean circulation patterns. PS2185 and the IODP Leg 302 cores are marked with a star on the Lomonosov Ridge. Kara Sea samples are represented by the triangles. The dashed arrows indicate the inflow of Atlantic near surface and intermediate waters from the Nordic Seas. An eastern branch flows across the Barents Sea, while a western branch flows along the western Svalbard margin. The solid arrows indicate the general circulation of the Arctic Intermediate Water (Rudels et al., 2004). This map is drawn based on the International Bathymetric Chart of the Arctic Ocean (IBCAO).

and mixing (Zimmermann et al., 2009a, b; Godfrey et al., 2009; Rickli et al., 2009, 2010; Stichel et al., 2012), as well as intensity and regime of past continental weathering, a signature produced by weathering-induced fractionation processes of Hf isotopes (van de Flierdt et al., 2002, 2007; Bayon et al., 2006, 2009). Past variations of the combined Hf–Nd isotope compositions of seawater have so far only been reconstructed from coarse resolution long term records obtained from ferromanganese crusts (Lee et al., 1999; Piotrowski et al., 2000; David et al., 2001; van de Flierdt et al., 2002, 2004a, b; Frank et al., 2006). Millennial scale resolution reconstructions of weathering regimes and water mass mixing applying past Hf–Nd isotope variations have so far been hampered by the lack of suitable analytical methods to extract seawater Hf isotope compositions from marine sediments. The leaching methods routinely applied for extracting seawater Nd and Pb isotope compositions (e.g. Bayon et al., 2002; Haley et al., 2008a) do not work for Hf isotopes due to the re-adsorption of the

seawater-derived Hf to the detrital phase during leaching (Gutjahr, 2006).

Previous work (Haley et al., 2008a) investigating past Nd isotope signatures of AIW revealed much more radiogenic values during glacial times ($\varepsilon_{Nd} > -7$) than today (ε_{Nd}: about -10.8). In fact, Icelandic basalts (located near the site of "headwaters" of North Atlantic inflow) and the Putorana flood basalts of Siberia are the only two possible sources to release radiogenic Nd and Hf to the central Arctic (Fig. 1). For various reasons including distance and general flow patterns, the Icelandic basalts were previously suggested a highly unlikely source for more radiogenic glacial Nd isotope compositions of AIW (Haley et al., 2008a). The Putorana flood basalts of Siberia remain the only major source able to supply radiogenic Nd isotope signatures to AIW. Therefore, radiogenic Nd isotope signatures of AIW in glacial times was interpreted as intrusion of significant amounts of dense brines carrying radiogenic Nd isotope compositions especially in the

Kara Sea region during periods of extensive continental glaciation on Siberia. The early shift of the Nd isotopes of AIW towards less radiogenic signatures at about 50 ka was then explained by the absence of a land based ice cover in the Kara Sea region after 50 ka including the LGM (cf. Svendsen et al., 2004). While a viable mechanism for the transfer of radiogenic shelf Nd isotope signatures to water masses around 1000 m deep where AIW prevailed has been provided by Haley et al. (2008a), there were no Nd isotope signatures from the Kara Sea shelf available. Therefore, the relative contribution between North Atlantic inflow and Kara Sea shelf input could not be well constrained.

A combined reconstruction of Hf–Nd isotope compositions of past central Arctic Intermediate Water (AIW) from authigenic, early diagenetic Fe–Mn oxyhydroxide of marine sediment is presented in this study. The investigations were carried out applying a modified leaching method of Gutjahr et al. (2007) and Haley et al. (2008a) to high-resolution central Arctic combined box/kastenlot core PS2185 (87° 31.9' N; 144° 22.9' E; 1,051 m water depth) and to Integrated Ocean Drilling Program (IODP) Leg 302 (a composite record of cores M0002 and M0004, 87°5 N, 137° E; 1,250 m water depth, Expedition "ACEX", thereafter referred to as Leg 302 core). Both PS2185 and Leg 302 cores were recovered on the Lomonosov Ridge (Fig. 1), for which well-developed age models are available (Spielhagen et al., 2004; Backman et al., 2008). Moreover, in order to better constrain the radiogenic isotope endmember signatures of the Siberian Arctic, five core-top samples from the Kara Sea were also analyzed for Nd and Hf isotope compositions (Fig. 1).

2. Materials and methods

Detailed published information about the stratigraphy and composition of the sediments of core PS2185 can be found in Spielhagen et al. (2004). The location, sedimentary features, and age model of Leg 302 core have been presented in Moran et al. (2006) and Backman et al. (2008). The sedimentation rates of the upper part of the Leg 302 core were constrained using cosmogenic ^{10}Be. Due to a recent revision of the half-life of ^{10}Be from 1.51 Myr to 1.387 Myr (Chmeleff et al., 2010; Korschinek et al., 2010), the age model for the uppermost 151 m of the Leg 302 core previously dated to cover the past 12.3 million years (Frank et al., 2008) had to be revised and is applied here for all data. The revised sedimentation rate for the upper 151 m is now 15.75 m/Myr resulting in an age of only 11.3 Ma at 151 m core depth, including a hiatus of 2 Myr duration between 135 and 140 m core depth. Within uncertainties this revised chronological information is still consistent with the few other independent biostratigraphic age constraints available (Backman et al., 2008). Two core-top sediment samples from the Lomonosov Ridge were measured to prove the seawater origin of the extracted Hf isotope compositons.

Approximately one gram of bulk sediment per sample is needed to guarantee the extraction of sufficient amounts of seawater-derived Hf (> 50 ng) for high precision isotope measurements. After washing samples three times with Milli-Q water, Nd and Hf contained in the sedimentary oxyhydroxide fraction were leached for about one hour in a single step using a dilute reducing and complexing solution consisting of 0.005 M hydroxylamine hydrochloride, 1.5% acetic acid, and 0.03 M Na-EDTA, buffered to pH=4 with suprapur® NaOH. A buffered acetic acid leach step was omitted since these sediments are essentially devoid of carbonates. The hydroxylamine hydrochloride and acetic acid mixture was 10-fold diluted compared with the method of Gutjahr et al. (2007) in order to avoid any potential contamination caused by leaching of clay minerals. To keep the extracted Hf in solution, we added 0.03 M Na-EDTA to the

leaching solution for complexing the Hf following Gutjahr (2006), which yielded 50–100 ng authigenic Hf per gram of bulk sediment. After centrifugation, the leach solution was decanted, evaporated, and processed through a cation exchange resin AG 50WX8 to separate and purify Nd and Hf. The Nd and Hf cuts were further separated from the other REEs, ytterbium and lutetium, respectively, with Ln-spec resin (Pin and Zalduegui, 1997; Münker et al., 2001). In order to constrain the origin of the detrital particles, prior to total dissolution of the detrital fraction, the previously leached sediments were leached again for about 24 h with a stronger leaching solution (0.05 M hydroxylamine hydrochloride) to ensure complete removal of residual Fe–Mn oxyhydroxides following the method applied in Gutjahr et al. (2007) and Haley et al. (2008a). Then the detrital samples were treated in aqua regia mixed with concentrated HF on a hotplate before complete dissolution in concentrated HNO_3 and HF in steel jacketed autoclaves at ~180–200 °C for 3–4 days. Subsequent separation and purification of the Nd and Hf followed the same procedures as described above.

The procedural blank for both elements was negligible (less than 1% and 0.2% contribution for Hf and Nd, respectively). Hafnium and Nd isotope ratios were measured on a 'Nu instruments' MC-ICP-MS at GEOMAR. Instrumental bias was corrected applying an exponential mass fractionation law using $^{146}Nd/^{144}Nd$ of 0.7219 and $^{179}Hf/^{177}Hf$ of 0.7325, respectively. To monitor the external reproducibility and system drift, generally four to six samples were bracketed by analyses of the standard JMC 475 and an internal laboratory standard solution (CertiPUR) for Hf isotopes, and of standard JNdi-1 and an internal laboratory standard (SPEX) for Nd isotopes. $^{176}Hf/^{177}Hf$ results were normalized to JMC475=0.282160 (Nowell et al., 1998) while $^{143}Nd/^{144}Nd$ results were normalized to JNdi-1=0.512115 (Tanaka et al., 2000). The 2σ external reproducibility of repeated standard measurements was 0.21 (n=28) and 0.30 (n=28) epsilon units for Hf and Nd isotopes, respectively.

3. Results

The Hf and Nd isotope data obtained from leachates and detrital fractions are provided in Table 1. The Fe–Mn oxyhydroxide based ε_{Nd} (− 10.6, − 10.8) and ε_{Hf} (+0.4,+0.4) reproduced present day AIW (ε_{Nd}: about − 10.8, ε_{Hf}: about +0.6, Andersson et al., 2008; Porcelli et al., 2009; Zimmermann et al., 2009a) as shown by leaching of two core-top samples on the Lomonosov Ridge (PS2185 and PS70/316, which is a location close to core PS2185). Three water samples at the core of AIW around 1000 m seem to have lower ε_{Hf} (+0.3, − 0.4, and − 1.4, Zimmermann et al., 2009a). Given that the analytical uncertainties of the Hf isotope data in their study were very high (± 2 to 3 epsilon units), an unambiguous comparison of the Hf isotope signatures between core-top leachates and modern AIW remains difficult. It is however noted that the modern ε_{Hf} of AIW of about +0.6 was suggested to be the likely present day Atlantic inflow signature (Zimmermann et al., 2009a) which dominates the modern AIW. Without better constraints, modern AIW ε_{Hf} of about +0.6 is thus used here. The Kara Sea sediment leachates have isotope signatures similar to the Ob and Yenisei rivers (ε_{Nd}: − 6.1 ± 0.3, − 5.2 ± 0.3 and ε_{Hf}: +1.5 ± 1.3, +3.0 ± 1.3, respectively), whereas the detrital fractions from Kara Sea sediments are clearly less radiogenic (ε_{Nd}: − 7.8 to − 8.5; ε_{Hf}: − 3.6 to − 14.2). The down core Nd-Hf isotope records from the Lomonosov Ridge show remarkably closely coupled trends. Two sets of isotopic records on millennial (Fig. 2, the Late Quaternary record) and million year (Fig. 3, the Neogene record) time scales were obtained.

Table 1
Nd-Hf isotopes from leachates and detrital materials of the Arctic sediments.

Sample[a]	Depth (m)	Age (Ma)	Leachate ^{143}Nd/^{144}Nd (2σ)	$ε_{Nd}$[b]	Haley et al.[c]	Leachate ^{176}Hf/^{177}Hf (2σ)	$ε_{Hf}$[d]	Detrital ^{143}Nd/^{144}Nd (2σ)	$ε_{Nd}$[b]	Detrital ^{176}Hf/^{177}Hf (2σ)	$ε_{Hf}$[d]
PS2179–1	coretop	0.000	0.512093 ± 4	−10.6	−10.5	0.282780 ± 3	0.4	0.512073 ± 4	−11.0	0.282529 ± 4	−8.5
PS70\316	coretop	0.000	0.512085 ± 4	−10.8		0.282780 ± 3	0.4				
duplicate run			0.512094 ± 4	−10.6							
PS2185–3	0.03	0.005	0.512077 ± 4	−10.9	−10.8	0.282766 ± 3	−0.1				
duplicate run			0.512089 ± 5	−10.7							
PS2185–3	0.08	0.009	0.512070 ± 5	−11.1	−10.8	0.282715 ± 3	−1.9	0.512082 ± 4	−10.9	0.282547 ± 3	−7.9
duplicate run			0.512070 ± 4	−11.1							
PS2185–3	0.10	0.013	0.512088 ± 7	−10.7	−10.5	0.282720 ± 3	−1.7				
PS2185–3	0.12	0.017	0.512077 ± 5	−10.9	−11.0	0.282719 ± 5	−1.8				
PS2185–3	0.16	0.032	0.512093 ± 5	−10.6	−10.7	0.282740 ± 2	−1.0				
PS2185–3	0.21	0.039	0.512086 ± 4	−10.8	−10.7	0.282742 ± 3	−1.0				
PS2185–3	0.26	0.046	0.512088 ± 5	−10.7	−10.6	0.282737 ± 3	−1.1				
PS2185–3	0.31	0.050	0.512247 ± 5	−7.6	−7.8	0.282842 ± 3	2.6				
PS2185–3	0.36	0.051	0.512257 ± 4	−7.4	−7.4	0.282831 ± 2	2.2	0.512193 ± 4	−8.7	0.282514 ± 2	−9
PS2185–6	0.69	0.055	0.512162 ± 4	−9.3		0.282731 ± 3	−1.4				
PS2185–6	0.95	0.060	0.512221 ± 4	−8.1	−7.3	0.282793 ± 3	0.8				
PS2185–6	1.13	0.063	0.512204 ± 5	−8.5		0.282783 ± 4	0.5				
PS2185–6	1.25	0.067	0.512140 ± 5	−9.7		0.282768 ± 3	0.0	0.512061 ± 5	−11.3	0.282513 ± 3	−9.1
PS2185–6	1.35	0.069	0.512174 ± 3	−9.0		0.282770 ± 3	0.1				
PS2185–6	1.45	0.071	0.512138 ± 3	−9.7		0.282774 ± 3	0.2				
PS2185–6	1.61	0.075	0.512136 ± 3	−9.8		0.282814 ± 3	1.6				
duplicate run			0.512134 ± 3	−9.8							
PS2185–6	1.81	0.081	0.512156 ± 3	−9.4		0.282730 ± 2	−1.4				
duplicate run			0.512159 ± 4	−9.3							
PS2185–6	2.05	0.093	0.512092 ± 3	−10.7		0.282711 ± 3	−2.0				
duplicate run			0.512098 ± 4	−10.5							
PS2185–6	2.21	0.105	0.512104 ± 3	−10.4		0.282670 ± 2	−3.5	0.512074 ± 4	−11.0	0.282486 ± 3	−10
PS2185–6	2.41	0.122	0.512180 ± 4	−8.9	−10.3	0.282742 ± 3	−1.0				
PS2185–6	2.56	0.137	0.512341 ± 4	−5.8		0.282872 ± 3	3.6				
PS2185–6	2.7	0.149	0.512291 ± 4	−6.8		0.282796 ± 3	1.0				
PS2185–6	2.78	0.156	0.512274 ± 3	−7.1	−6.5	0.282813 ± 3	1.5	0.512195 ± 4	−8.6	0.282462 ± 3	−11
PS2185–6	3.01	0.179	0.512239 ± 4	−7.8		0.282785 ± 3	0.6				
PS2185–6	3.15	0.183	0.512134 ± 4	−9.8		0.282726 ± 3	−1.5				
PS2185–6	3.41	0.217	0.512111 ± 4	−10.3		0.282731 ± 2	−1.3				
PS2185–6	3.51	0.231	0.512128 ± 4	−10.0		0.282753 ± 3	−0.6				
PS2185–6	3.59	0.243	0.512138 ± 5	−9.7	−10.0	0.282718 ± 3	−1.8	0.512091 ± 4	−10.7	0.282492 ± 4	−9.8
PS2185–6	3.61	0.250	0.512153 ± 4	−9.5		0.282725 ± 3	−1.6				
PS2185–6	3.67	0.273	0.512178 ± 4	−9.0	−9.8	0.282737 ± 2	−1.1				
PS2185–6	3.73	0.295	0.512176 ± 4	−9.0	−7.8	0.282750 ± 3	−0.7				
PS2185–6	3.83	0.316	0.512153 ± 4	−9.5		0.282749 ± 3	−0.7				
duplicate run			0.512150 ± 4	−9.5							
4/3/2/143–145	10.81	0.686	0.512152 ± 4	−9.5	−10.3	0.282735 ± 3	−1.2	0.512034 ± 6	−11.8	0.282489 ± 4	−9.9
duplicate run			0.512144 ± 3	−9.6							
4/4/1/110–112	13.69	0.869	0.512192 ± 4	−8.7	−8.0	0.282755 ± 3	−0.5				
duplicate run			0.512196 ± 4	−8.6							
2/5/1/100–102	21.42	1.360	0.512252 ± 5	−7.5	−9.3	0.282776 ± 3	0.2				
2/5/2/50–52	22.43	1.424	0.512268 ± 4	−7.2	−6.3	0.282790 ± 3	0.7	0.512043 ± 5	−11.6	0.282424 ± 2	−12
2/7/2/52–54	31.14	1.977	0.512174 ± 4	−9.1	−8.2	0.282717 ± 2	−1.8				
2/10/2/70–72	43.76	2.778	0.512193 ± 4	−8.7	−8.0	0.282720 ± 2	−1.7	0.512024 ± 7	−12.0	0.282420 ± 4	−12
2/11/3/70–72	49.70	3.156	0.512163 ± 3	−9.3	−8.3	0.282739 ± 3	−1.1	0.512022 ± 4	−12.0	0.282445 ± 3	−12
2/14/1/80–82	60.80	3.860	0.512232 ± 3	−7.9	−7.5	0.282768 ± 2	0.0				
2/19/1/25–27	81.45	5.171	0.512215 ± 4	−8.2	−7.6	0.282767 ± 3	−0.1				
2/20/2/70–72	88.41	5.613	0.512219 ± 3	−8.2	−7.2	0.282773 ± 2	0.2				
2/25/1/78–80	110.99	7.047	0.512239 ± 4	−7.8	−6.9	0.282790 ± 3	0.8	0.512086 ± 6	−10.8	0.282455 ± 3	−11

Table 1 (continued)

Sample[a]	Depth (m)	Age (Ma)	Leachate $^{143}Nd/^{144}Nd$ (2σ)	ε_{Nd}[b]	Haley et al.[c]	ε_{Hf}[d]	Leachate $^{176}Hf/^{177}Hf$ (2σ)	ε_{Nd}[b]	Detrital $^{143}Nd/^{144}Nd$ (2σ)	Detrital $^{176}Hf/^{177}Hf$ (2σ)	ε_{Hf}[d]
2/29/2/70–72	130.40	8.279	0.512207 ± 3	−8.4	−8.2	−0.4	0.282757 ± 2	−10.7	0.512089 ± 7	0.282497 ± 2	−9.6
2/35/2/78–80	155.05	11.527	0.512224 ± 3	−8.1	−7.6	−0.1	0.282767 ± 2			0.282511 ± 5	−9.1
2/40/2/80–82	175.38	12.818	0.512176 ± 4	−9.0	−8.7	0.8	0.282792 ± 3				
2/43/2/70–72	189.68	13.726	0.512202 ± 4	−8.5	−9.4	−0.4	0.282758 ± 2				
BP97-12	coretop	0.000	0.512338 ± 5	−5.9		2.7	0.282845 ± 3	−7.8	0.512236 ± 4	0.282667 ± 3	−3.6
BP97-32	coretop	0.000	0.512357 ± 5	−5.5		5.2	0.282916 ± 3	−7.8	0.512237 ± 6	0.282653 ± 3	−4.1
BP97-46	coretop	0.000	0.512337 ± 5	−5.9		3.9	0.282879 ± 4	−8.1	0.512222 ± 4	0.282546 ± 3	−7.9
BP97-52	coretop	0.000	0.512325 ± 4	−6.1		3.1	0.282856 ± 5	−8.2	0.512219 ± 4	0.282367 ± 3	−14.2
BP97-56	coretop	0.000	0.512333 ± 5	−6.0		3.5	0.282869 ± 4	−8.5	0.512201 ± 5	0.282374 ± 3	−14.0

[a] PS2185 and the nearby core-top samples PS2179-1, PS70.316 were from combined box/kastenlot cores taken in the central Arctic (Spielhagen et al., 2004). IODP Leg 302 samples in this study were recovered from drill cores M0002A and M0004C (Expedition 302 Scientists, 2005). The BP97 sediment samples were taken by Bettina Finkenberger (GEOMAR) in 1997 during an expedition with RV Akademik Boris Petrov to the Kara Sea.

[b] $\varepsilon_{Nd} = [(^{143}Nd/^{144}Nd)_{sample}/(^{143}Nd/^{144}Nd)_{CHUR} - 1]*10^4$; where $(^{143}Nd/^{144}Nd)_{CHUR} = 0.512638$ (Jacobsen and Wasserburg, 1980).

[c] comparison with previously published neodymium isotope data from Haley et al. (2008a).

[d] $\varepsilon_{Hf} = [(^{176}Hf/^{177}Hf)_{sample}/(^{176}Hf/^{177}Hf)_{CHUR} - 1]*10^4$; where $(^{176}Hf/^{177}Hf)_{CHUR} = 0.282769$ (Nowell et al., 1998).

In the Late Quaternary record, more radiogenic ε_{Hf} signatures are observed during glacial MIS 4, 6, but no resolvable change in MIS 8 which may be due to the lower time resolution for this part of the record (Fig. 2). While the ε_{Nd} signature of AIW remained virtually unchanged over the past 50 kyr, the ε_{Hf} signature of AIW decreased from −1.0 at 30 ka to −1.9 until the early Holocene and then became more radiogenic to reach the ε_{Hf} signature of +0.4 at the present day. The most significant excursion on the order of seven ε_{Hf} units from +4.0 to −3.1 occurred at the end of MIS 6. The ε_{Nd} evolution of AIW resembles the pattern of ε_{Hf} very closely albeit at smaller amplitude. No noticeable phase lag has been found between the two isotope systems at the studied time resolution. This similarity also holds for the Neogene (14 to 2 Myr, Fig. 3), during which ε_{Nd} and ε_{Hf} varied between −11.1 and −5.8 and between −3.5 and +3.6, respectively. Both the Nd and Hf isotopic records displayed only relatively small variations prior to 4 Ma and thereafter became overall less radiogenic and more variable. During the early Pleistocene, the ε_{Hf} signal shifted back to +0.7 at 1.7 Ma before decreasing again to −1.2 at 0.8 Ma. It is likely that further high-resolution variations occurred and have been missed in the early Pleistocene record because of the lower time resolution in this part of our record. Overall, the Nd isotopes showed a smaller range of variability than the Hf isotopes on the Myr timescale. These leachate data are within the range of data defined by Arctic seawater samples in ε_{Nd} versus ε_{Hf} space (Fig. 4), but are below the seawater array (Albarède et al., 1998) defined by global seawater and slow-growing Fe–Mn nodule and crust data.

For comparison, the Hf and Nd isotope compositions of the detrital fractions in several sediment samples were measured to investigate the detrital provenance and the leaching efficiency in terms of selectively dissolving the authigenic, seawater-derived phase only. The detrital fractions have significantly less radiogenic isotope signatures than those of the Fe–Mn oxyhydroxide phase (Figs. 2–4). The detrital ε_{Hf} signature in central Arctic sediments ranges from −7.9 to −12.3 and the average ε_{Hf} difference between the leached and detrital fraction is about 10 ε_{Hf} units. In fact, the $\varepsilon_{Hf}-\varepsilon_{Nd}$ signatures of the bulk sediments from the central Arctic as well as from the Kara Sea are indistinguishable from the terrestrial array (Fig. 4).

4. Discussion

4.1. The leached Hf isotope compositions: reliable record of past bottom water signatures?

It has been demonstrated that the Nd isotope compositions of bulk sediment leachates in various abyssal marine settings represent a seawater signal, except for locations with a presence of volcanic ash (e.g. Piotrowski et al., 2005; Gutjahr et al., 2008; Haley et al., 2008a, Elmore et al., 2011). However, it has yet to be demonstrated that this is also the case for the extracted Hf isotope compositions. Using a similar method as described above, Gutjahr (2006) presented Hf isotope records obtained from the authigenic Fe–Mn oxyyhydroxide fraction of Blake Ridge sediments, and suggested that seawater-derived Hf can be extracted from marine sediments. However, the Hf concentration in the leachates was generally very low, and although systematically higher than the detrital fraction, Hf/Al were not as clearly distinguishable from the detrital fraction as in the case of Nd/Al or Pb/Al (Gutjahr, 2006). Due to the low concentration of Hf in the authigenic fraction, the mass balance approach taken in Gutjahr et al. (2007) cannot be reliably applied to assess potential offsets of authigenic ε_{Hf} signatures by contributions from partial dissolution of detrital material. Nevertheless, several lines of evidences
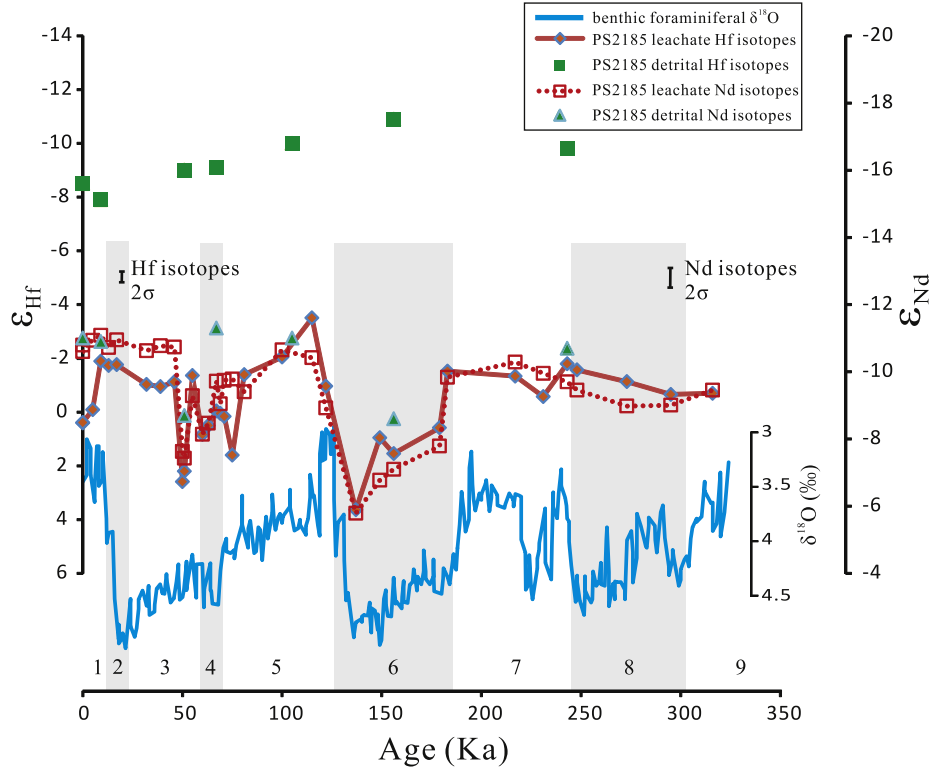
Fig. 2. Late Quaternary Nd (dashed line and open squares)—Hf (solid line and full diamonds) isotopic evolution of Arctic Intermediate Water obtained from core PS2185. Glacial–interglacial cycles of Nd and Hf isotopes are compared with the globally stacked benthic foraminiferal $\delta^{18}O$ data (Zachos et al., 2001). Gray bands correspond to the glacial isotope stages. Also shown are Hf–Nd isotope compositions of the detrital fraction in this core. The axis dimensions for Nd and Hf isotopes are adjusted in order to demonstrate the close co-evolution of leachate Nd–Hf isotope signatures with the global benthic foraminiferal $\delta^{18}O$ evolution.
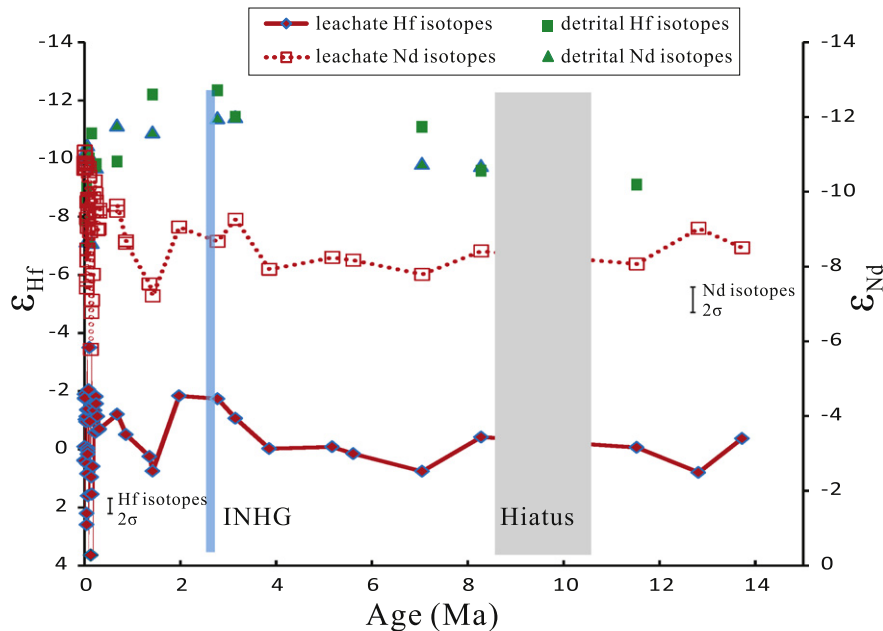
Fig. 3. Nd–Hf isotopic evolution of the Arctic Intermediate Water from the Middle Miocene to the present. Also shown are total dissolution data of the detrital fraction (triangles). The data are from both PS2185 (0–300,000 years) and IODP Leg 302 (0.7–13.7 million years). Note that the axis dimensions for Nd and Hf isotopes are different from Fig. 2. INHG denotes the time of major intensification of Northern Hemisphere Glaciation.

presented below corroborate that our leached Hf isotope compositions represent a bottom water signature.

First, the two core top samples yield Hf–Nd isotope signatures (Table 1) that are within error identical to previously determined

signatures in the Nansen, Amundsen, and Makarov Basins ($\varepsilon_{Nd}=$ -10.8, $\varepsilon_{Hf}= +0.6$ albeit with large uncertainty, Andersson et al., 2008; Porcelli et al., 2009; Zimmermann et al., 2009a), which have been suggested to represent the isotopic compositions of the
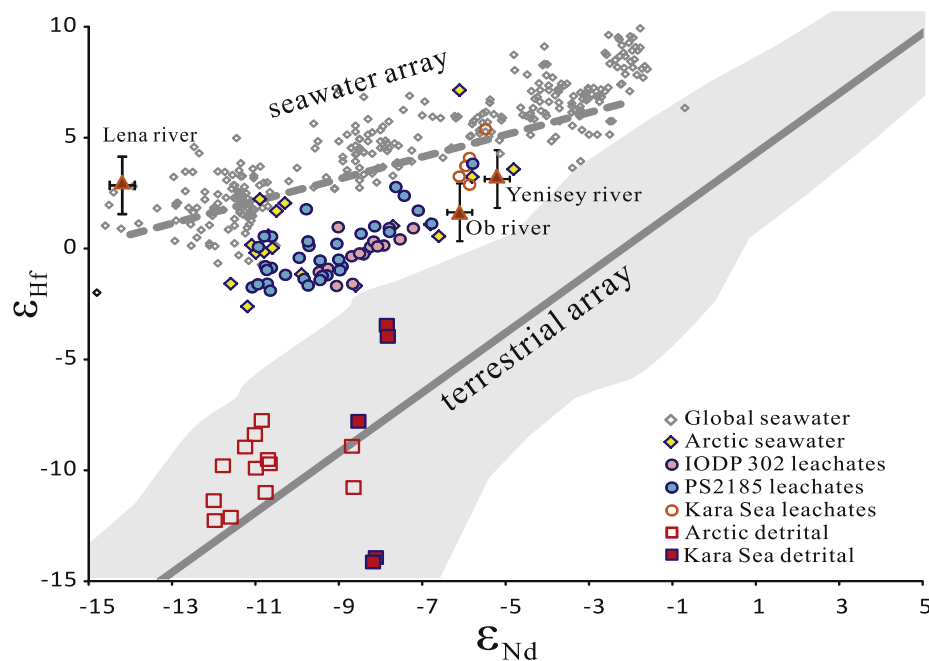
Fig. 4. Hafnium–neodymium isotope systematics of the leachates and detrital materials in this study together with previously published data and $\varepsilon_{Nd}-\varepsilon_{Hf}$ correlation lines from the literature. The gray shaded area denotes the terrestrial igneous rocks (van de Flierdt et al., 2004a). The data from leachates and Arctic seawater (Zimmermann et al., 2009a) are significantly above the terrestrial array (Vervoort et al., 1999), but still somewhat below the seawater array (Albarède et al., 1998). Global seawater Nd–Hf isotope data were obtained from hydrogenetic Fe–Mn crusts/nodules (Lee et al., 1999; Piotrowski et al., 2000; van de Flierdt et al., 2004a, b) and seawater dissolved component (< 0.45 μm, Rickli et al., 2009, 2010 Zimmermann et al., 2009a, b; Stichel et al., 2012). Data of the Arctic rivers are from Zimmermann et al., 2009a.

North Atlantic inflow (Zimmermann et al., 2009a). In addition, the Hf isotopic signatures of the downcore leachates are significantly more radiogenic than their corresponding detrital Hf isotope compositions. Moreover, the late Quaternary detrital Hf isotope signal fluctuated much less and did not vary in a fashion similar to the leached ε_{Hf} signatures (Fig. 2). Rather, the evolution of leached Hf isotope signatures was very similar to that of Nd isotopes. In Nd-Hf isotope space (Fig. 4), the leachates and detrital fractions fall into completely different areas. Finally, all the leachate data vary within the range of the modern Nd-Hf isotopic composition of Arctic seawater (Fig. 4). Together, these arguments lend strong support to our suggestion that the leached Hf isotope records shown here reliably represent a past seawater signal.

4.2. Consistency of detrital Nd–Hf isotope compositions of the Lomonosov Ridge sediments with the terrestrial array

While detrital ε_{Nd} signatures of present day Kara Sea sediments show very similar signatures ($\Delta\varepsilon_{Nd} \leq 0.6$), their ε_{Hf} signal varies widely ($\Delta\varepsilon_{Hf}$ reaches 10.6) (Fig. 4). This is explained by different portions of zircon in the sediment at different locations on the shelf as a consequence of some mineral and grain size sorting effects (Patchett et al., 1984; Carpentier et al., 2009; Bayon et al., 2009; Vervoort et al., 2011). The inhomogenous zircon distribution in these sediments is probably caused by the currents of the Kara Sea and the supply of material from different rock types in the hinterland. However, the detrital Hf–Nd isotope compositions from the more remote Lomonosov Ridge are close to the terrestrial array and display smaller Hf isotopic variations (Fig. 4). Therefore, their Hf–Nd isotope distribution likely reflected poor sorting of sediments during shelf sea ice or iceberg transport over the last 14 million years (Haley et al., 2008b), which is expected not to fractionate zircons significantly from the other minerals. Our interpretation is supported by the perennial sea ice conditions over the last 14 Myr in the Arctic Ocean (Darby, 2008; Frank et al., 2008; St. John, 2008; Polyak et al., 2010).

4.3. Subordinate role of weathering regime changes in driving the Hf isotopic evolution of AIW

Similar to Nd isotopes, the Hf isotope composition of AIW has been controlled by weathering contributions from different sources, distributed and mixed in dissolved form by the deep circulation. However, the release of Hf from these sources may also have depended on changes of the weathering regime. Zircon, as the main host mineral of Hf, is very resistant to weathering and contains highly unradiogenic Hf because of its very low Lu/Hf ratios. As a result, isotope compositions of Hf dissolved during weathering processes are generally more radiogenic than those of the bulk rocks (the "zircon effect", White et al., 1986; Albarède et al., 1998; van de Flierdt et al., 2002), although the zircon effect alone is probably not enough to produce the seawater trend in ε_{Nd} versus ε_{Hf} space (Chen et al., 2011). During glacial weathering, enhanced breakdown and dissolution of zircons may in turn potentially drive the dissolved Hf isotope signatures in seawater towards less radiogenic bulk rock isotope compositions (i.e., more congruent weathering), while Nd isotopes are not influenced significantly by these processes (van de Flierdt et al., 2002). The AIW record shows a very closely coupled evolution of Hf and Nd isotope compositions of AIW on both glacial-interglacial (Fig. 2), as well as on longer time scales (Fig. 3). For example, the late Quaternary changes can be related to processes mostly following glacial-interglacial time scales (except the data younger than 50 ka). Fig. 5 shows the late Quaternary variability of the Nd and Hf isotope data of AIW obtained from the PS2815 leachates for different marine isotopes stages. The interglacial stages are generally characterized by less radiogenic isotope compositions. MIS6 contains the most radiogenic isotope compositions that even approached the likely Kara Sea endmember of weathering inputs (Figs. 4 and 5) whereas the penultimate deglaciation witnessed the most abrupt drop both in Nd (5 ε units) and Hf isotope compositions (7 ε units) to less radiogenic values. Given the synchronous variations of Nd and Hf isotopes, changes in
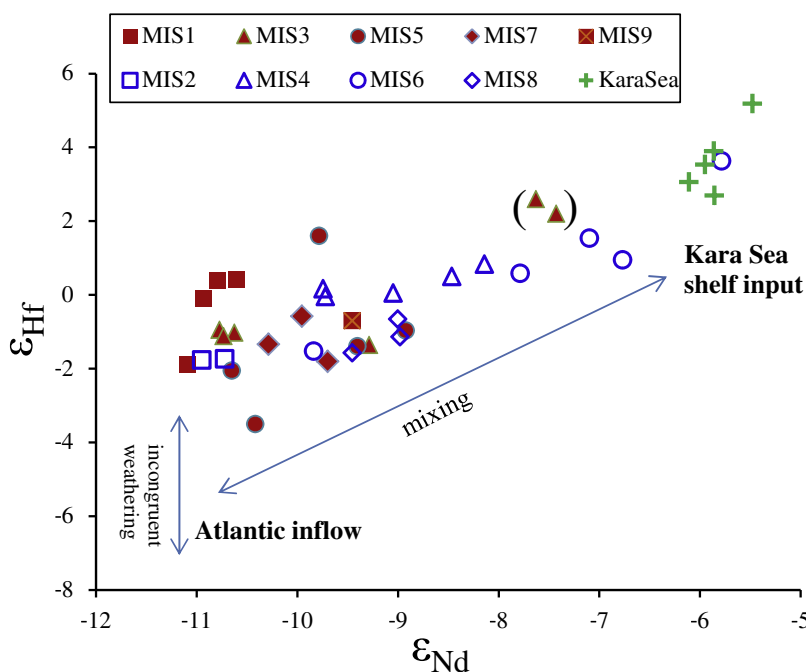
Fig. 5. Hafnium–neodymium isotope systematics of the leachates obtained from core PS2185 at different marine isotope stages. Also shown are the data of Kara Sea surface sediment leachates. The isotopic variation of PS2185 can be interpreted as mainly reflecting a two-component mixing between the Atlantic inflow and radiogenic input from the Kara Sea shelf (oblique arrow), while incongruent weathering (vertical arrow) seems to only play a subordinate role.

weathering regime have obviously only played a subordinate role in driving the Hf isotopic evolution of AIW.

4.4. Variations of North Atlantic inflow to AIW over the past 14 Myr

4.4.1. Constraints on the sources of Nd and Hf in AIW

North Atlantic inflow today shows a relatively homogeneous and unradiogenic signature throughout the water column in its Nd isotope composition ($\varepsilon_{Nd} \sim -10.7$ to -10.8, Piepgras and Wasserburg, 1987; Lacan and Jeandel, 2004; Andersson et al., 2008), which precludes contributions from weathering or exchange with sediments near Iceland as a significant source of Nd. Reportedly, present day exchange with Iceland derived basaltic material does not affect the deep water ε_{Nd} signature of the main path of North Atlantic inflow but rather mainly influences the signature of southward flowing currents such as the East Greenland Current (Lacan and Jeandel, 2004). The same situation probably also holds for Hf, given that the average Hf isotope composition of Arctic deep water ($\varepsilon_{Hf} \sim 0.6$, Zimmermann et al., 2009a) is similar to the marginal North Atlantic surface water (-1 to 1.4, Rickli et al., 2009, 2010; Godfrey et al., 2009). Riverine inflow and shelf sediment-seawater exchange processes also contribute Nd and Hf to Arctic seawater (Andersson et al., 2008; Porcelli et al., 2009; Zimmermann et al., 2009a). As a consequence of these inputs into the semi-enclosed Arctic basin, the concentrations of Hf and Nd in the Arctic deep water are slightly elevated compared with the Atlantic inflow. Nevertheless, most of the deep and intermediate waters in the Nansen, Amundsen, and Makarov Basins have Nd-Hf isotope compositions very close to the Atlantic inflow, supporting the dominant source from the Atlantic waters. In the Canada Basin, where more radiogenic waters of Pacific origin (for both Nd and Hf, Porcelli et al., 2009; Zimmermann et al., 2009b) exert an influence via the Bering Strait, Nd and Hf isotopes are generally more radiogenic than in the other basins of Arctic Ocean. Thus, at first glance, it may seem reasonable to interpret the more radiogenic isotope signatures found in glacial times (Fig. 2) to reflect enhanced input

from the Pacific. However, this possibility can be excluded given that the Bering Strait inflow was already closed during incipient glaciation at a sea level about 50 m lower than today.

As mentioned in the introduction, the only major source for supplying radiogenic Nd (and probably also Hf) isotope compositions were the Putorana flood basalts of Siberia. All Nd–Hf leachate data obtained here fit within a mixing envelope between Kara Sea shelf input and North Atlantic waters (Figs. 4 and 5), supporting the assertion that both Nd and Hf isotopic variations can be explained by changing mixing proportions of the above two endmembers. The other potential sources around the Arctic, such as the Eastern Laptev Sea, North America and Greenland unlikely dominated the AIW signatures at the Lomonosov Ridge sampling site, mainly because of the lack of suitable transport mechanisms of water masses and detrital material from these sources to the studied area (Haley et al., 2008b). In addition, Nd–Hf isotopic compositions of these sources are not consistent with mixing relationships in Fig. 4 (for example the Eastern Laptev Sea shelf input, as represented by the Lena river signature, Zimmermann et al., 2009a).

4.4.2. Glacial reduction of North Atlantic inflow into the Arctic

The newly obtained record of Hf isotopic AIW records, as well as our constraints on the isotope compositions of inputs from the Kara Sea, allows a close look at the characteristics of changes in contributions between the two potential endmembers: Atlantic inflow and brines formed on the more radiogenic Eurasian shelf.

During the penultimate glacial period, the very radiogenic values both in ε_{Hf} (+3.6) and ε_{Nd} (−5.8) are essentially indistinguishable from the Kara Sea endmember values (Figs. 4 and 5). This suggests that the Atlantic inflow has almost completely lost its influence on the Nd-Hf isotope signature of AIW at the Lomonosov Ridge sampling site during this interval. We thus propose that at least during the penultimate glacial period, North Atlantic water inflow was significantly reduced compared to the modern situation.

One may argue that much more radiogenic isotope signatures of the brines could have formed on the Kara sea shelf during

glacial times. Consequently, high ε_{Hf} and ε_{Nd} of AIW in glacial times approaching the modern Kara sea endmember may not necessarily reflect changes in inflow flux of the North Atlantic. However, this is unlikely given the ε_{Nd} signatures of Kara Sea/ Laptev Sea shelf sediments were inferred to have been similar between modern time and glacial maxima (Tütken et al., 2002). In addition, Pb isotopic compositions of AIW imply that the late Quaternary Eurasian sediment weathering around the Arctic was generally more "congruent" than around the North Atlantic at least in terms of its Pb-specific chemical weathering behavior (Haley et al., 2008b; Kurzweil et al., 2010). Thus the isotopic composition of Kara Sea input most likely did not change significantly over glacial-interglacial periods. In fact, reduced glacial North Atlantic inflow (and its unradiogenic Nd and Hf isotopes) to the Arctic Ocean is consistent with previous studies from the Arctic Ocean. From stable isotopes and microfossil abundances in a number of Arctic Ocean deep-sea cores, it was shown that strong Atlantic Water advection was restricted to interglacials and interstadials of the last 200 ky (Spielhagen et al., 2004). Moreover, cyclic variations in color and manganese content in sediments from the central Arctic Ocean also imply decreased ventilation of the Arctic Ocean during glacial times (Jakobsson et al., 2000; März et al., 2011).

However, the actual glaciation history on the Eurasian continent through time has been variable (Svendsen et al., 2004) and has not been directly coupled with global ice sheet volume inferred from benthic foraminifera (Fig. 2). In this regard, the global benthic oxygen isotope variations in Fig. 2 rather serve as a global climatic reference frame for the data presented in our study. From about 30 ka to the LGM, the Fennoscandian ice sheet expanded towards the shelf edge in the Nordic Seas (Ottesen et al., 2008; Mangerud et al., 2011), thereby transporting glacially eroded material to the continental margin off Northwest Europe. The Hf isotope composition of the North Atlantic inflow may potentially have been modified along the pathway of the inflow by exchange processes between these glacial sediments and seawater and/or by brine injection from sea ice formation at the ice sheet margin. As Nd isotope compositions through this period were virtually invariable, the Hf isotope variability was most likely controlled by incongruent weathering. This is demonstrated by the increasingly congruent weathering signature carried by the North Atlantic inflow from about 30 ka to the early Holocene, i.e., ε_{Hf} signature of AIW decreased from -1.0 at 30 ka to -1.9 at 9 ka. During the Holocene, the North Atlantic inflow was enhanced (e.g., Slubowska et al., 2005), whereas the weathering regime of the sediments along the inflow path became more incongruent (i.e., release of more radiogenic Hf). This inference is consistent with our record, in which the ε_{Hf} signature of AIW became more radiogenic in the Holocene while the ε_{Nd} signature remained stable. Nevertheless, because of the complex erosional and glaciation history of the high latitude Eurasian continent, it is worthy to note that Hf isotope fractionation induced by incongruent weathering might not always have responded linearly to the orbital scale glacial-interglacial cycles. In other words, interglacial marine isotope stages may not always correspond to more incongruent weathering than glacial isotope stages around the Arctic.

4.5. The Neogene leachate record and weathering regime of the high latitude Eurasian continent

We suggest that the intermediate and comparatively stable Hf isotope signatures during most of the Neogene period (Fig. 3) reflects relatively steady contributions from North Atlantic inflow and brine formation in the Kara sea region. Since around 4 Ma, the Hf and Nd isotope signatures have varied at higher amplitude (Fig. 3), probably as a consequence of more pronounced glacial/ interglacial cycles.

Water mass exchange between the North Atlantic and the Arctic may already have occurred as early as the Eocene (Gleason et al., 2009; Poirier and Hillaire-Marcel, 2011) and should not have been tectonically restricted any more since the full opening of the Fram Strait for deep water exchange 17.5 million years ago (Jakobsson et al., 2007). However, the inflow of Atlantic water volumetrically similar to the present day situation, which was likely linked to the development of a far north-reaching Norwegian Current, may only have started as late as the mid Pleistocene (1.1–1.0 Ma, Thiede et al., 1998). This early suggestion is consistent with the Nd–Hf isotope data presented here, given that ε_{Nd} signatures essentially identical to the Atlantic endmember were only observed during the interglacials of the late Quaternary. Therefore, the dominant role of Atlantic inflow for the deep and intermediate Arctic Ocean may only be a relatively recent phenomenon.

Similar to modern Arctic seawater, most of the leachate data are plotted significantly above the terrestrial array (Vervoort et al., 1999) but still below the seawater array as defined by the data from other ocean basins (Fig. 4, Albarède et al., 1998). According to Piotrowski et al. (2000) and van de Flierdt et al. (2002), glacial weathering regimes on the continents are needed to explain such an offset. Thus these data suggest that glacial climatic conditions linked to preferentially physical weathering regimes dominated the past 14 Myr. IRD (ice rafted debris) records and surface morphology of sand-sized quartz from Leg 302 core sediments also indicated that the ice-house conditions, probably initiated as early as the mid-Eocene, were able to support growth of land-based ice sheets around the Arctic margin throughout our studied period of time (St. John, 2008). Due to the restricted connection of the Arctic "Mediterranean" ocean basin and the relatively short residence time of Hf in seawater on the order of a few hundred years (Rickli et al., 2009), the remaining global ocean was not affected by these weathering regimes and the global seawater data were characterized by less congruent weathering (van de Flierdt et al., 2002). Consequently, according to our data, the intensification of Northern Hemisphere glaciation at about 2.7 Ma (e.g. Raymo, 1994) did not result in significant changes of weathering inputs around the Arctic Ocean. In this respect, weathering regime changes after the onset of NHG that led to more radiogenic Pb isotope compositions and a deviation of Hf isotope compositions toward the "terrestrial Nd-Hf isotope array (see Fig. 4)" of the North Atlantic were most likely dominated by inputs from Greenland and Canada (von Blanckenburg and Nägler, 2001; van de Flierdt et al., 2002), rather than the Eurasian continental margin.

5. Conclusions

A first combined Nd–Hf isotopic record has been obtained from the authigenic Fe–Mn oxyhydroxide fraction of two sediment cores recovered in the central Arctic. The remarkably close coupling of the evolution of the two radiogenic isotope records, the overall systematic variations, and the agreement between core top data with modern seawater suggest that seawater-derived Hf isotope compositions can be reliably extracted from marine sediments. An observed offset of Nd and Hf isotopic compositions from the seawater array, which has also been observed from previous Arctic seawater analyses, is probably the result of a prevailing glacial weathering regime around the Arctic Ocean since at least 14 Myr ago. The data obtained in this study are explained by radiogenic Hf and Nd inputs originating mainly from the Kara Sea shelf area and a severely restricted inflow of waters from the North Atlantic in glacial time. During

MIS6, the most radiogenic isotope compositions of both Nd and Hf essentially approached the Kara sea shelf endmember compositions, indicating an essentially ceased Atlantic inflow to the central Arctic. However, the intensity of North Atlantic inflow has been weaker during most of the Neogene than during late Quaternary interglacial times. This study demonstrates that authigenic Hf isotopes extracted from marine sediments are a potentially powerful proxy for continental weathering inputs, as well as for water mass mixing in high resolution paleoceanographic studies.

Acknowledgments

Appendix A. Supporting information

Supplementary data associated with this article can be found in the online version at http://dx.doi.org/10.1016/j.epsl.2012.08.012.

References

Andersson, P.S., Porcelli, D., Frank, M., Bjork, G., Dahlqvist, R., Gustafsson, O., 2008. Neodymium isotopes in seawater from the Barents Sea and Fram Strait Arctic–Atlantic gateways. Geochim. Cosmochim. Acta 72, 2854–2867.

Aagaard, K., Swift, J.H., Carmack, E.C., 1985. Thermohaline circulation in the Arctic mediterranean seas. J. Geophys. Res. 90, 4833–4846.

Albarède, F., Simonetti, A., Vervoort, J.D., Blichert-Toft, J., Abouchami, W., 1998. A Hf–Nd isotopic correlation in ferromanganese nodules. Geophys. Res. Lett. 25, 3895–3898.

Backman, J., Jakobsson, M., Frank, M., Sangiorgi, F., Brinkhuis, H., Stickley, C., O'Regan, M., Lovlie, R., Palike, H., Spofforth, D., Gattacecca, J., Moran, K., King, J., Heil, C., 2008. Age model and core-seismic integration for the Cenozoic Arctic Coring Expedition sediments from the Lomonosov Ridge. Paleoceanography 23, PA1S03, http://dx.doi.org/10.1029/2007PA001476.

Bayon, G., German, C.R., Boella, R.M., Milton, J.A., Taylor, R.N., Nesbitt, R.W., 2002. An improved method for extracting marine sediment fractions and its application to Sr and Nd isotopic analysis. Chem. Geol. 187, 179–199.

Bayon, G., Burton, K.W., Soulet, G., Vigier, N., Dennielou, B., Etoubleau, J., Ponzevera, E., German, C.R., Nesbitt, R.W., 2009. Hf and Nd isotopes in marine sediments: constraints on global silicate weathering. Earth Planet. Sci. Lett. 277, 318–326.

Bayon, G., Vigier, N., Burton, K.W., Brenot, A., Carignan, J., Etoubleau, J., Chu, N.C., 2006. The control of weathering processes on riverine and seawater hafnium isotope ratios. Geology 34, 433–436.

Carpentier, M., Chauvel, C., Maury, R.C., Mattielli, N., 2009. The "zircon effect" as recorded by the chemical and Hf isotopic compositions of Lesser Antilles forearc sediments. Earth Planet. Sci. Lett. 287, 86–99.

Chen, T.-Y., Ling, H.-F., Frank, M., Zhao, K.-D., Jiang, S.-Y., 2011. Zircon effect alone insufficient to generate seawater Nd-Hf isotope relationships. Geochem. Geophys. Geosyst. 12, Q05003, http://dx.doi.org/10.1029/2010GC003363.

Chmeleff, J., von Blanckenburg, F., Kossert, K., Jakob, D., 2010. Determination of the (10)Be half-life by multicollector ICP-MS and liquid scintillation counting. Nucl. Instrum. Meth. Phys. Res. B 268, 192–199.

Darby, D.A., 2008. Arctic perennial ice cover over the last 14 million years. Paleoceanography 23, PA1S07, http://dx.doi.org/10.1029/2007PA001479.

David, K., Frank, M., O'Nions, R.K., Belshaw, N.S., Arden, J.W., 2001. The Hf isotope composition of global seawater and the evolution of Hf isotopes in the deep Pacific Ocean from Fe–Mn crusts. Chem. Geol. 178, 23–42.

Elmore, A.C., Piotrowski, A.M., Wright, J.D., Scrivner, A.E., 2011. Testing the extraction of past seawater Nd isotopic composition from North Atlantic deep sea sediments and foraminifera. Geochem. Geophys. Geosyst. 12, Q09008 http://dx.doi.org/10.1029/2011gc003741.

Expedition 302 Scientists, 2005. Arctic Coring Expedition (ACEX): paleoceanographic and tectonic evolution of the central Arctic Ocean. IODP Preliminary Report., 302. http://dx.doi.org/10.2204/iodp.pr.302.2005.

Frank, M., Marbler, H., Koschinsky, A., de Flierdt, T.V., Klemm, V., Gutjahr, M., Halliday, A.N., Kubik, P.W., Halbach, P., 2006. Submarine hydrothermal venting related to volcanism in the Lesser Antilles: evidence from ferromanganese precipitates. Geochem. Geophys. Geosyst. 7, Q04010, http://dx.doi.org/10.1029/2005gc001140.

Frank, M., Backman, J., Jakobsson, M., Moran, K., O'Regan, M., King, J., Haley, B.A., Kubik, P.W., Garbe-Schönberg, D., 2008. Beryllium isotopes in central Arctic Ocean sediments over the past 12.3 million years: stratigraphic and paleoclimatic implications. Paleoceanography 23, PA1S02, http://dx.doi.org/10.1029/2007PA001478.

Gleason, J.D., Thomas, D.J., Moore, T.C., Blum, J.D., Owen, R.M., Haley, B.A., 2009. Early to middle Eocene history of the Arctic Ocean from Nd–Sr isotopes in fossil fish debris, Lomonosov Ridge. Paleoceanography 24, PA2215, http://dx.doi.org/10.1029/2008pa001685.

Godfrey, L.V., Zimmermann, B., Lee, D.C., King, R.L., Vervoort, J.D., Sherrell, R.M., Halliday, A.N., 2009. Hafnium and neodymium isotope variations in NE Atlantic seawater. Geochem. Geophys. Geosyst. 10, Q08015, http://dx.doi.org/10.1029/2009GC002508.

Gutjahr, M., 2006. Reconstruction of changes in ocean circulation and continental weathering using radiogenic isotopes in marine sediments. Swiss Federal Institute of Technology Zürich.

Gutjahr, M., Frank, M., Stirling, C.H., Keigwin, L.D., Halliday, A.N., 2008. Tracing the Nd isotope evolution of North Atlantic deep and intermediate waters in the Western North Atlantic since the Last Glacial Maximum from Blake Ridge sediments. Earth Planet. Sci. Lett. 266, 61–77.

Gutjahr, M., Frank, M., Stirling, C.H., Klemm, V., van de Flierdt, T., Halliday, A.N., 2007. Reliable extraction of a deepwater trace metal isotope signal from Fe–Mn oxyhydroxide coatings of marine sediments. Chem. Geol. 242, 351–370.

Haley, B.A., Frank, M., Spielhagen, R.F., Eisenhauer, A., 2008a. Influence of brine formation on Arctic Ocean circulation over the past 15 million years. Nat Geosci 1, 68–72.

Haley, B.A., Frank, M., Spielhagen, R.F., Fietzke, J., 2008b. Radiogenic isotope record of Arctic Ocean circulation and weathering inputs of the past 15 million years. Paleoceanography 23, PA1S13, http://dx.doi.org/10.1029/2007PA001486.

Jacobsen, S.B., Wasserburg, G.J., 1980. Sm–Nd isotopic evolution of chondrites. Earth Planet. Sci. Lett. 50, 139–155.

Jakobsson, M., Lovlie, R., Al-Hanbali, H., Arnold, E., Backman, J., Morth, M., 2000. Manganese and color cycles in Arctic Ocean sediments constrain Pleistocene chronology. Geology 28, 23–26.

Jakobsson, M., Backman, J., Rudels, B., Nycander, J., Frank, M., Mayer, L., Jokat, W., Sangiorgi, F., O'Regan, M., Brinkhuis, H., King, J., Moran, K., 2007. The Early Miocene onset of a ventilated circulation regime in the Arctic Ocean. Nature 447, 986–990.

Karcher, M.J., Oberhuber, J.M., 2002. Pathways and modification of the upper and intermediate waters of the Arctic Ocean. J. Geophys. Res.-Oceans, 107.

Korschinek, G., Bergmaier, A., Faestermann, T., Gerstmann, U.C., Knie, K., Rugel, G., Wallner, A., Dillmann, I., Dollinger, G., von Gostomski, C.L., Kossert, K., Maiti, M., Poutivtsev, M., Remmert, A., 2010. A new value for the half-life of (10)Be by Heavy-Ion Elastic Recoil Detection and liquid scintillation counting. Nucl. Instrum. Meth. Phys. Res. B 268, 187–191.

Kurzweil, F., Gutjahr, M., Vance, D., Keigwin, L., 2010. Authigenic Pb isotopes from the Laurentian Fan: changes in chemical weathering and patterns of North American freshwater runoff during the last deglaciation. Earth Planet. Sci. Lett. 299, 458–465.

Lacan, F., Jeandel, C., 2004. Neodymium isotopic composition and rare earth element concentrations in the deep and intermediate Nordic Seas: constraints on the Iceland Scotland Overflow Water signature. Geochem. Geophys. Geosyst. 5, Q11006, http://dx.doi.org/10.1029/2004GC000742.

Lee, D.C., Halliday, A.N., Hein, J.R., Burton, K.W., Christensen, J.N., Gunther, D., 1999. Hafnium isotope stratigraphy of ferromanganese crusts. Science 285, 1052–1054.

Mangerud, J., Gyllencreutz, R., Lohne, Ø, Svendsen, J.I., 2011. Glacial History of Norway. In: Ehlers, J., Gibbard, P.L., Hughes, P.D. (Eds.), Developments in Quaternary Science, Vol. 15. Amsterdam, The Netherlands, pp. 279–298.

März, C., Stratmann, A., Matthiessen, J., Meinhardt, A.K., Eckert, S., Schnetger, B., Vogt, C., Stein, R., Brumsack, H.J., 2011. Manganese-rich brown layers in Arctic Ocean sediments: composition, formation mechanisms, and diagenetic overprint. Geochim. Cosmochim. Acta 75, 7668–7687.

Moran, K., Backman, J., Brinkhuis, H., Clemens, S.C., Cronin, T., Dickens, G.R., Eynaud, F., Gattacceca, J., Jakobsson, M., Jordan, R.W., Kaminski, M., King, J., Koc, N., Krylov, A., Martinez, N., Matthiessen, J., McInroy, D., Moore, T.C., Onodera, J., O'Regan, M., Paelike, H., Rea, B., Rio, D., Sakamoto, T., Smith, D.C., Stein, R., John, K.S., Suto, I., Suzuki, N., Takahashi, K., Watanabe, M., Yamamoto, M., Farrell, J., Frank, M., Kubik, P., Jokat, W., Kristoffersen, Y., 2006. The Cenozoic palaeoenvironment of the Arctic Ocean. Nature 441, 601–605.

Münker, C., Weyer, S., Scherer, E., Mezger, K., 2001. Separation of high field strength elements (Nb, Ta, Zr, Hf) and Lu from rock samples for MC-ICPMS measurements. Geochem. Geophys. Geosyst. 2, 1064, http://dx.doi.org/10.1029/2001GC000183.

Nowell, G.M., Kempton, P.D., Noble, S.R., Fitton, J.G., Saunders, A.D., Mahoney, J.J., Taylor, R.N., 1998. High precision Hf isotope measurements of MORB and OIB by thermal ionisation mass spectrometry: insights into the depleted mantle. Chem. Geol. 149, 211–233.

Ottesen, D., Stokes, C.R., Rise, L., Olsen, L., 2008. Ice-sheet dynamics and ice streaming along the coastal parts of northern Norway. Quaternary Sci. Rev. 27, 922–940.

Patchett, P.J., White, W.M., Feldmann, H., Kielinczuk, S., Hofmann, A.W., 1984. Hafnium Rare-Earth element fractionation in the sedimentary system and crustal recycling into the earth's mantle. Earth Planet. Sci. Lett. 69, 365–378.

Piepgras, D.J., Wasserburg, G.J., 1987. Rare-Earth Element Transport in the Western North-Atlantic Inferred from Nd Isotopic Observations. Geochim. Cosmochim. Acta 51, 1257–1271.

Pin, C., Zalduegui, J.F.S., 1997. Sequential separation of light rare-earth elements, thorium and uranium by miniaturized extraction chromatography: application to isotopic analyses of silicate rocks. Anal. Chim. Acta 339, 79–89.

Piotrowski, A.M., Goldstein, S.L., Hemming, S.R., Fairbanks, R.G., 2005. Temporal Relationships of Carbon Cycling and Ocean Circulation at Glacial Boundaries. Science 307, 1933–1938.

Piotrowski, A.M., Lee, D.C., Christensen, J.N., Burton, K.W., Halliday, A.N., Hein, J.R., Günther, D., 2000. Changes in erosion and ocean circulation recorded in the Hf isotopic compositions of North Atlantic and Indian Ocean ferromanganese crusts. Earth Planet. Sci. Lett. 181, 315–325.

Poirier, A., Hillaire-Marcel, C., 2011. Improved Os-isotope stratigraphy of the Arctic Ocean. Geophys. Res. Lett. 38, L14607, http://dx.doi.org/10.1029/2011GL047953.

Polyak, L., Alley, R.B., Andrews, J.T., Brigham-Grette, J., Cronin, T.M., Darby, D.A., Dyke, A.S., Fitzpatrick, J.J., Funder, S., Holland, M., Jennings, A.E., Miller, G.H., O'Regan, M., Savelle, J., Serreze St., M., John, K., White, J.W.C., Wolff, E., 2010. History of sea ice in the Arctic. Quaternary Sci. Rev. 29, 1757–1778.

Porcelli, D., Andersson, P.S., Baskaran, M., Frank, M., Björk, G., Semiletov, I., 2009. The distribution of neodymium isotopes in Arctic Ocean basins. Geochim. Cosmochim. Acta 73, 2645–2659.

Raymo, M.E., 1994. The Initiation of Northern-Hemisphere Glaciation. Annu. Rev Earth Planet Sci 22, 353–383.

Rickli, J., Frank, M., Halliday, A.N., 2009. The hafnium-neodymium isotopic composition of Atlantic seawater. Earth Planet. Sci. Lett. 280, 118–127.

Rickli, J., Frank, M., Baker, A.R., Aciego, S., de Souza, G., Georg, R.B., Halliday, A.N., 2010. Hafnium and neodymium isotopes in surface waters of the eastern Atlantic Ocean: implications for sources and inputs of trace metals to the ocean. Geochim. Cosmochim. Acta 74, 540–557.

Rudels, B., Jones, E.P., Anderson, L.G., Kattner, G., 1994. On the intermediate depth waters of the Arctic Ocean. In: Johannessen, O.M., Muench, R.D., Overland, J.E. (Eds.), The Polar Oceans and Their Role in Shaping the Global Environment. American Geophysical Union, Washington, DC, pp. 33–46.

Rudels, B., Jones, E.P., Schauer, U., Eriksson, P., 2004. Atlantic sources of the Arctic Ocean surface and halocline waters. Polar Res. 23, 181–208.

Slubowska, M.A., Koc, N., Rasmussen, T.L., Klitgaard-Kristensen, D., 2005. Changes in the flow of Atlantic water into the Arctic Ocean since the last deglaciation: evidence from the northern Svalbard continental margin, 80 degrees N. Paleoceanography 20, PA4014, http://dx.doi.org/10.1029/2005PA001141.

Spielhagen, R.F., Baumann, K.H., Erlenkeuser, H., Nowaczyk, N.R., Nørgaard-Pedersen, N., Vogt, C., Weiel, D., 2004. Arctic Ocean deep-sea record of northern Eurasian ice sheet history. Quaternary Sci. Rev. 23, 1455–1483.

Spielhagen, R.F., Werner, K., Sorensen, S.A., Zamelczyk, K., Kandiano, E., Budeus, G., Husum, K., Marchitto, T.M., Hald, M., 2011. Enhanced Modern Heat Transfer to the Arctic by Warm Atlantic Water. Science 331, 450–453.

Stichel, T., Frank, M., Rickli, J., Haley, B.A., 2012. The hafnium and neodymium isotope composition of seawater in the Atlantic sector of the Southern Ocean. Earth Planet. Sci. Lett. 317–318, 282–294.

St. John, K., 2008. Cenozoic ice-rafting history of the central Arctic Ocean: terrigenous sands on the Lomonosov Ridge. Paleoceanography 23, PA1S05 http://dx.doi.org/10.1029/2007PA001483.

Svendsen, J.I., Alexanderson, H., Astakhov, V.I., Demidov, I., Dowdeswell, J.A., Funder, S., Gataullin, V., Henriksen, M., Hjort, C., Houmark-Nielsen, M., Hubberten, H.W., Ingolfsson, O., Jakobsson, M., Kjaer, K.H., Larsen, E., Lokrantz, H., Lunkka, J.P., Lysa, A., Mangerud, J., Matiouchkov, A., Murray, A., Moller, P., Niessen, F., Nikolskaya, O., Polyak, L., Saarnisto, M., Siegert, C., Siegert, M.J., Spielhagen, R.F., Stein, R., 2004. Late quaternary ice sheet history of northern Eurasia. Quaternary Sci. Rev. 23, 1229–1271.

Tanaka, T., Togashi, S., Kamioka, H., Amakawa, H., Kagami, H., Hamamoto, T., Yuhara, M., Orihashi, Y., Yoneda, S., Shimizu, H., Kunimaru, T., Takahashi, K., Yanagi, T., Nakano, T., Fujimaki, H., Shinjo, R., Asahara, Y., Tanimizu, M., Dragusanu, C., 2000. JNdi-1: a neodymium isotopic reference in consistency with LaJolla neodymium. Chem. Geol. 168, 279–281.

Thiede, J., Winkler, A., Wolf-Welling, T., Eldholm, O., Myhre, A.M., Baumann, K.H., Henrich, R., Stein, R., 1998. Late Cenozoic history of the Polar North Atlantic: results from ocean drilling. Quaternary Sci. Rev. 17, 185–208.

Tütken, T., Eisenhauer, A., Wiegand, B., Hansen, B.T., 2002. Glacial-interglacial cycles in Sr and Nd isotopic composition of Arctic marine sediments triggered by the Svalbard/Barents Sea ice sheet. Mar. Geol. 182, 351–372.

van de Flierdt, T., Frank, M., Lee, D.C., Halliday, A.N., 2002. Glacial weathering and the hafnium isotope composition of seawater. Earth Planet. Sci. Lett. 198, 167–175.

van de Flierdt, T., Frank, M., Lee, D.C., Halliday, A.N., Reynolds, B.C., Hein, J.R., 2004a. New constraints on the sources and behavior of neodymium and hafnium in seawater from Pacific Ocean ferromanganese crusts. Geochim. Cosmochim. Acta 68, 3827–3843.

van de Flierdt, T., Frank, M., Halliday, A.N., Hein, J.R., Hattendorf, B., Gunther, D., Kubik, P.W., 2004b. Tracing the history of submarine hydrothermal inputs and the significance of hydrothermal hafnium for the seawater budget-a combined Pb–Hf–Nd isotope approach. Earth Planet. Sci. Lett. 222, 259–273.

van de Flierdt, T., Goldstein, S.L., Hemming, S.R., Roy, M., Frank, M., Halliday, A.N., 2007. Global neodymium-hafnium isotope systematics—revisited. Earth Planet. Sci. Lett. 259, 432–441.

Vervoort, J.D., Patchett, P.J., Blichert-Toft, J., Albarède, F., 1999. Relationships between Lu–Hf and Sm–Nd isotopic systems in the global sedimentary system. Earth Planet. Sci. Lett. 168, 79–99.

Vervoort, J.D., Plank, T., Prytulak, J., 2011. The Hf–Nd isotopic composition of marine sediments. Geochim. Cosmochim. Acta 75, 5903–5926.

von Blanckenburg, F., Nägler, T.F., 2001. Weathering versus circulation-controlled changes in radiogenic isotope tracer composition of the Labrador Sea and North Atlantic Deep Water. Paleoceanography 16, 424–434.

White, W.M., Patchett, J., Benothman, D., 1986. Hf Isotope Ratios of Marine-Sediments and Mn Nodules - Evidence for a Mantle Source of Hf in Seawater. Earth Planet. Sci. Lett. 79, 46–54.

Zachos, J., Pagani, M., Sloan, L., Thomas, E., Billups, K., 2001. Trends, rhythms, and aberrations in global climate 65 Ma to present. Science 292, 686–693.

Zhang, J., Rothrock, D.A., Steele, M., 1998. Warming of the Arctic Ocean by a strengthened Atlantic Inflow: model results. Geophys. Res. Lett. 25, 1745–1748.

Zimmermann, B., Porcelli, D., Frank, M., Andersson, P.S., Baskaran, M., Lee, D.C., Halliday, A.N., 2009a. Hafnium isotopes in Arctic Ocean water. Geochim. Cosmochim. Acta 73, 3218–3233.

Zimmermann, B., Porcelli, D., Frank, M., Rickli, J., Lee, D.C., Halliday, A.N., 2009b. The hafnium isotope composition of Pacific Ocean water. Geochim. Cosmochim. Acta 73, 91–101.